Appl Phys B (2010) 99: 53–62
DOI 10.1007/s00340-010-3912-2

Applied Physics B
Lasers and Optics

# Picosecond diode-pumped 1.5 μm Er,Yb:glass lasers operating at 10–100 GHz repetition rate

**A.E.H. Oehler · M.C. Stumpf · S. Pekarek · T. Südmeyer · K.J. Weingarten · U. Keller**

Received: 7 January 2010 / Published online: 6 February 2010


**Abstract** Stable ultrafast laser sources at multi-GHz repetition rates are important for various application areas, such as optical sampling, frequency comb metrology, or advanced high-speed return-to-zero telecom systems. We review SESAM-mode-locked Er,Yb:glass lasers operating in the 1.5 μm spectral region at multi-GHz repetition rates, discussing the key improvements that have enabled increasing the repetition rate up to 100 GHz. We also present further improved results with shorter pulse durations from a 100 GHz Er,Yb:glass laser. With an improved SESAM design we achieved 1.1 ps pulses with up to 30 mW average output power. Moreover, we discuss for the first time the importance of beam quality deteriorations arising from frequency-degenerate higher order spatial modes in such lasers.

## 1 Introduction

There are numerous applications for multi-GHz laser sources in science and technology such as optical clocking [1], photonic switching [2] or high-speed electro-optic sampling [3], just to mention a few. Multi-GHz mode-locked lasers emitting in the 1.5 μm spectral range are particularly interesting for fiber-optical telecommunication applications as they operate in the window of minimal glass absorption, which enables long-haul data transfer. Pulsed lasers with high repetition rates are important tools for advanced high-speed return-to-zero (RZ) data transmission systems [4], typically operating at 40 Gbit/s or higher: data streams are encoded on the pulse train with a modulator, which then only has to change its state between two successive pulses. This approach reduces the highly stringent demands of the modulator, as the pulse shaping is already done by the laser source. In current state-of-the-art high bit-rate systems, the pulsed laser source usually runs at a much lower repetition rate and needs to be time multiplexed to the desired frequency. A pulse source directly operating at the system frequency with high average output power can greatly simplify the system design, as the multiplexing device as well as the amplifiers can be omitted. In addition to their excellent properties in the time domain, which in telecom applications are especially important for optical-time-division-multiplexing (OTDM) systems, mode-locked lasers also generate a stable comb-shaped spectrum in the frequency domain. The comb lines of this spectrum, which are the phase-locked longitudinal modes of the laser, are equidistantly spaced, with the spacing being determined by the repetition rate of the laser. Therefore mode-locked GHz-lasers are multi-wavelength sources that can be used for wavelength-division-multiplexing (WDM) systems [5]. Besides telecom applications, GHz frequency combs are highly anticipated for direct frequency comb spectroscopy [6], as they offer high spectral power per comb line leading to an increased SNR for precision frequency measurements. Also applications such as optical clocks [7] or the frequency comb calibration of high-resolution astronomical spectrographs [8–10] benefit from GHz frequency combs. All of these applications have in common that they require a pulse source which is compact, affordable and reliable in operation. Furthermore the pulse source should exhibit low noise

A.E.H. Oehler · M.C. Stumpf · S. Pekarek · T. Südmeyer · U. Keller (✉)
Institute of Quantum Electronics, Department of Physics, ETH Zurich, Wolfgang-Pauli-Strasse 16, 8093 Zürich, Switzerland
e-mail: keller@phys.ethz.ch

A.E.H. Oehler · K.J. Weingarten
Time-Bandwidth Products AG, Technoparkstrasse 1, 8005 Zürich, Switzerland

and timing jitter and emit close to transform limited pulses with a high extinction ratio and the ability to set or tune the wavelength in the regime of interest.

The great interest in 1.5 μm laser sources with tens of GHz repetition rate provided a strong motivation for numerous different approaches to develop and improve lasers generating such pulse trains. Some examples are harmonically mode-locked fiber lasers [11], hybrid mode-locked edge-emitting semiconductor lasers [12], passively mode-locked VECSEL (Vertical External Cavity Surface Emitting Laser) [13] or synchronously pumped monolithic optical parametric oscillators (OPO) [14]. Diode-pumped, passively mode-locked Er,Yb:glass lasers offer an excellent alternative to these other approaches. Due to their miniature cavities, they are compact, they can be pumped by standard telecom diodes and only need a low-cost gain medium and a semiconductor saturable absorber mirror (SESAM) [15–17]. Because their pulse generation is entirely passive, no high frequency electronics are required. Although their basic design is very simple, numerous challenges had to be overcome to obtain high repetition rate operation, like the design of very compact stable laser cavities or the development of suitable saturable absorbers. For a long time it was believed that passive mode-locking of a solid state laser at GHz repetition rates is not possible [18] or at least impractically difficult. This was mainly due to the strong tendency of solid state lasers to Q-switched mode-locking, which is mainly a result of the long upper state lifetimes and high gain saturation values of solid state gain materials [19]. A major breakthrough was the demonstration of the first passively, fundamentally mode-locked 10 GHz Er,Yb:glass laser in 2002 [20]. Since then, a deeper understanding of the Q-switching dynamics [21, 22] and the consequent exploitation of the design flexibility of SESAMs [23] have led to fundamentally mode-locked 1.5 μm lasers with repetition rates up to 100 GHz [24].

This paper reviews the designs and the obtained results of passively mode-locked Er,Yb:glass lasers operating in the 1.5 μm spectral region with repetition rates up to 100 GHz. In addition, we present new results on reducing the pulse duration of a 100 GHz laser with optimized SESAM dispersion, achieving 1.1 ps pulses with up to 35 mW average output power. We also discuss beam quality deteriorations arising from frequency-degenerate higher order spatial modes, which are presented for the first time for high repetition rate lasers. We conclude with a summary and an outlook towards monolithic integration.

## 2 Experimental setups and results

The main challenge in designing a passively mode-locked laser operating at high repetition rates is to overcome the Q-switching-mode-locking (QML) threshold, above which stable cw mode-locking is achieved. With the general stability criterion against Q-switching proposed by Hönninger et al. [19]

$$\left(\frac{P_{\text{intra}}}{f_{\text{rep}}}\right)^2 > F_{\text{sat,L}} A_{\text{eff,L}} F_{\text{sat,A}} A_{\text{eff,A}} \Delta R \tag{1}$$

(with $P_{\text{intra}}$ being the intracavity power, $f_{\text{rep}}$ the laser repetition rate, $F_{\text{sat}}$ the saturation fluence and $A_{\text{eff}}$ the effective mode area in the laser gain medium (L) and on the absorber (A) respectively) it is apparent that achieving stable mode-locking becomes more challenging with increasing $f_{\text{rep}}$. Although this stability criterion is strictly speaking not valid for high repetition rate lasers, as some of the assumptions made to derive (1) are not fulfilled for multi-GHz lasers, it still can be used to obtain some useful design guidelines. For a more detailed discussion on the influence of additional effects on the QML-threshold such as two-photon absorption or incomplete recovery of the absorber, refer to [22, 25, 26]. Nevertheless (1) reveals the engineering parameters which can be used to obtain stable mode-locking: the effective mode areas $A_{\text{eff,L}}$ in the gain medium and $A_{\text{eff,L}}$ on the absorber, which can be influenced by the cavity design of the laser, and the parameters of the saturable absorber, namely the modulation depth $\Delta R$ and the saturation fluence $F_{\text{sat,A}}$. Equation (1) implies that the effective mode areas should be minimized while the saturable absorber should exhibit low saturation fluence together with a reasonably low modulation depth.

### 2.1 Er,Yb:glass lasers with up to 50 GHz repetition rate

Starting from well-known solid state laser cavities operating in the MHz repetition rate range, achieving GHz repetition rates with fundamental mode-locking requires that the length of the optical resonator has to be substantially reduced. As an example, the resonator length of a 10-GHz standing-wave cavity in air is about 15 mm and consequently only about 3 mm for a 50 GHz laser. Our approach is a miniature V-shaped cavity, with the gain medium sitting in a beam waist between two curved dielectric mirrors. One of these mirrors is the output coupler with a transmission between 0.5% and 1.3%, the second one is a folding mirror, providing a second beam waist on the SESAM which is used as the cavity end-mirror (Fig. 1, left). The SESAM is mounted on a piezo-element enabling us to fine-tune the repetition rate of the laser over several MHz with a precision in the range of 1 kHz (both values depend on the fundamental repetition rate). The gain glass is end-pumped either through the cavity folding mirror or alternatively through the output coupler by a fiber-coupled laser diode. In the latter case we place an additional dichroic mirror in the pump beam to separate the laser output from the pump. To reduce losses and

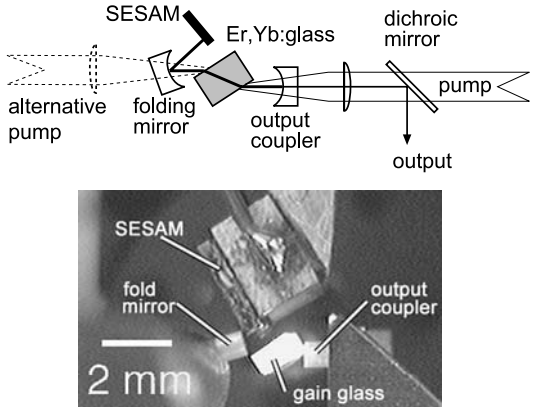


**Fig. 1** Experimental setup for a V-shaped 10-50 GHz Er,Yb:glass laser cavity [27]. Schematic (*top*) and photograph of a 50 GHz laser (*bottom*). As shown in the schematic, different pumping options are possible, depending on the clear aperture of the mirrors

parasitic reflections and therefore maintain a high-Q cavity, the uncoated gain glass is inserted in a flat-flat configuration under Brewster's angle. This also ensures linearly polarized laser operation. With increasing repetition rate, the thickness of the gain element has to be reduced for geometrical reasons. To compensate for the shorter gain length, the doping concentrations are increased accordingly. The SESAMs have a saturation fluence of about 15 μJ/cm$^2$ and a modulation depth of approximately 0.4% typically.

With this cavity design we achieved repetition rates ranging from 10 up to 50 GHz with picoseconds pulses and average output powers from about 10 up to 30 mW [20, 27–30]. Figure 2 shows the spectral properties of a 50-GHz laser. The equidistantly spaced longitudinal modes can be clearly resolved with an optical spectrum analyzer (Fig. 2, top). The RF-spectrum (Fig. 2, bottom) confirms stable mode-locking as only a single peak and no frequency side bands are visible on the instrument-limited noise floor. More detailed results of the different lasers built with this design are listed in Table 1 in Sect. 2.4. Repetition rates higher than 50 GHz were not feasible with this approach mainly due to the extent of the gain element which is used at Brewster's angle thereby filling up most of the free space inside the cavity (Fig. 1, bottom). This prevents the cavity mirrors from being moved closer together.

### *2.1.1 Wavelength tuning*

The laser cavities up to a repetition rate of 25 GHz allow for the additional insertion of a solid 20 μm low-finesse etalon which enables wavelength-tuning of the laser emission. Because the transmission characteristics of the etalon reduces the effective gain bandwidth, a broadening of the pulse duration can be observed compared to the free running laser. To obtain a flatter gain profile and therefore maximize the accessible overall tuning range, the inversion level in the

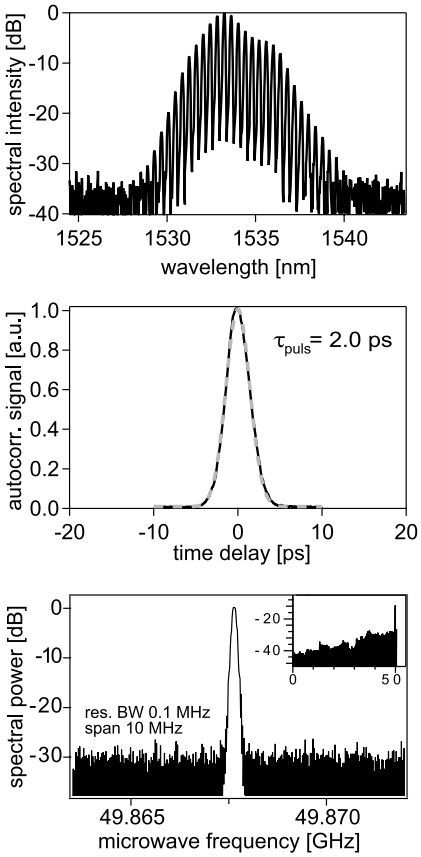


**Fig. 2** According to [27] we summarize here the properties of a 50 GHz laser: the optical spectrum (*top*, logarithmic scale) was measured with an optical spectrum analyzer with a resolution bandwidth of 0.01 nm. *Middle*: Autocorrelation trace together with fit-curve (*grey, dashed*) for ideal sech$^2$ pulses. The pulse repetition rate was measured with a fast photodiode and an RF-spectrum analyzer (*bottom*); the *inset* shows no sidebands, indicating clean fundamental mode-locking

gain element is well adjusted [31], using a 1.3% output coupler. Figure 3 shows the pulse-width and the average output power together with the generated optical spectra of a 12.5 GHz laser as an example for the tuning behavior of a high repetition rate Er,Yb:glass laser. The laser can be continuously tuned from 1528 to 1563 nm, which covers almost the entire telecom C-band, while the pulse durations of 1.7 to 2.7 ps is sufficiently short for many telecom applications at this frequency.

## 2.2 Er,Yb:glass laser with 80 GHz repetition rate

To overcome the geometrical limitations preventing higher repetition rates, a new cavity-design was developed. With the gain medium as the main limiting factor, the shape of the Er,Yb:glass was changed to a triangular geometry such that it could be used in a flat-Brewster configuration. Together with a flat output coupler on a wedged substrate, the overall cavity length could be reduced by 35%. In addition we reduced the size of the curved folding mirror to a diameter

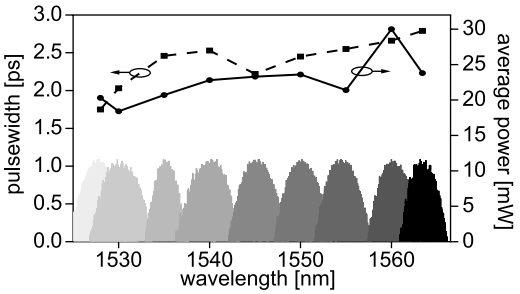


**Fig. 3** Tuning performance of a 12.5 GHz laser: pulse duration (*dashed*) and average output power (solid) is plotted for nine different etalon angles versus the resulting emission wavelength. *Bottom* (*grey shaded*): respective optical spectra

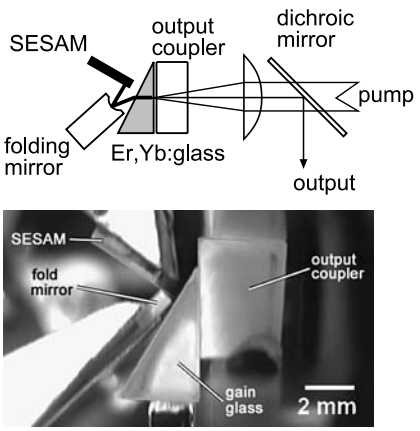


**Fig. 4** Experimental setup for a 77 GHz laser cavity: schematic (*top*) and photograph (*bottom*) [32]

of 0.7 mm with a clear aperture of about 0.6 mm. Note that the small gap between the gain glass and the output coupler, which acts as an air-spaced etalon, can be used to tune the emission-wavelength of the laser.

With this cavity design a repetition rate of 77 GHz in 3-ps pulses and an average output power of 10.7 mW was achieved [32]. Figure 5 shows the optical spectrum and the autocorrelation of the generated pulses.

Normally we would use a fast photodiode with a microwave spectrum analyzer to determine the repetition rate of a laser, however such devices operating to beyond 50 GHz were not available for this work. Therefore the repetition rate was determined with an autocorrelator from Femtochrome Research Inc. (model FR-103MN) by measuring the distance between the peaks of the autocorrelation and the first cross-correlations. The autocorrelator uses a rotating prism-pair as its varying delay arm, which is not internally compensated to provide a completely linear time scale at its analog output. If a large time-window is measured, some deviations from linearity have to be corrected. To calibrate the autocorrelator, we used a laser with 200 fs pulses at 1.5 µm wavelength to measure the temporal shift of the pulse peak

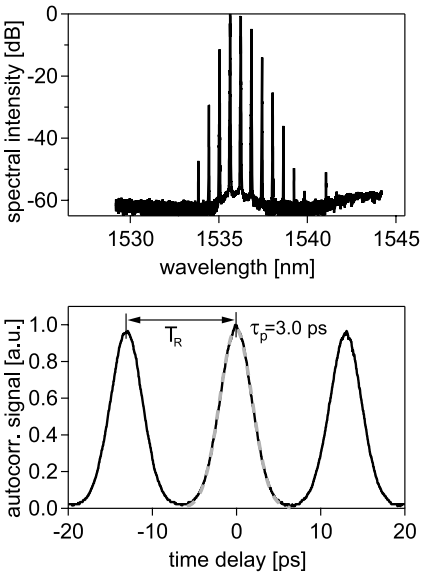


**Fig. 5** According to [32] we summarize here the properties of a 77 GHz laser: optical spectrum (*top*, logarithmic scale) of the laser output. Autocorrelation trace (*bottom, solid*) together with fit-curve for ideal 3-ps $\mathrm{sech}^2$ pulse train (*grey, dashed*) [32]. The repetition rate of the laser is determined by measuring the distance $T_R$ between the autocorrelation- and the cross-correlation peaks

position with respect to the length of the fixed delay arm. We could fit this dependence with a 2nd order polynomial to avoid an error of 10% over a scan length of 40 ps compared to a linear fit.

### 2.3 Record-high repetition rate of 101 GHz from an Er,Yb:glass laser

To further increase the repetition rate to beyond 100 GHz, the 80 GHz cavity design was further modified (s. Fig. 6, top right). Because the gain medium with its refractive index of 1.53 fills a large portion of the folded resonator, reducing the overall cavity length to about 1.26 mm, we use a partially monolithic approach: the output coupler coating with 1% transmission was directly applied to the flat side of the gain medium. In addition we implemented changes in the geometry of the gain glass and the folding mirror. Gain length, folding angle and mode sizes are adapted for stable cw mode-locking. The overall pump geometry remains unchanged. With the new setup, we initially reached a repetition rate of 90 GHz in 4.1-ps pulses and an average output power of 10 mW [33]. Only by improving the surface quality of the highly curved folding mirror (radius of curvature 0.5 mm) as well as the scattering properties of the dielectric coating, this result was further improved to get a record high repetition rate of 101.5 GHz in 1.6-ps pulses at an average output power of 35 mW. This is a substantial advancement compared to the previous results. The optical properties of the laser output are shown in detail in Fig. 7. At such high

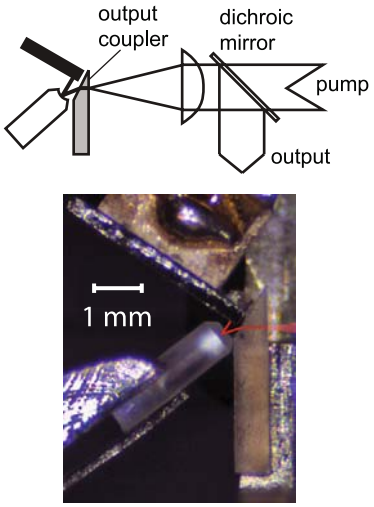


**Fig. 6** Experimental setup for the 101 GHz laser cavity: schematic (*top*) and photograph (*bottom*) [24]. The Er,Yb:glass is flat on one side, coated with a 1.2% output coupler and under Brewster's angle inside the cavity. The collimated pump beam is focused into the gain glass such that it is mode-matched to the laser mode. The output beam is collimated by the same lens. Both beams are separated afterwards by a dichroic mirror. OC: output coupler

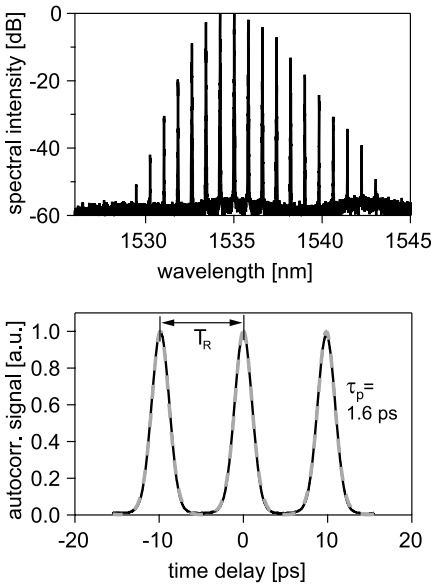


**Fig. 7** According to [24] we summarize here the properties of a 101-GHz laser. *Top*: optical spectrum (logarithmic scale). The mode separation is 0.8 nm. *Bottom*: autocorrelation trace including cross-correlations (*solid line*) with fit-curve using ideal $\mathrm{sech}^2$ pulses (*grey dashed line*). Cavity roundtrip time $T_R = 9.85$ ps. The pulses have a duration of 1.6 ps

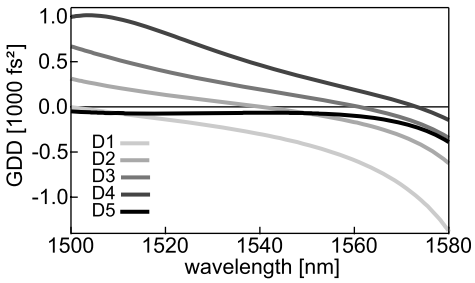


**Fig. 8** Calculated dispersion curves for different SESAM structures

repetition rates, the intracavity pulse energies become very low (around 35 pJ in the described laser). To suppress Q-switched mode-locking, a mode radius of about 15 µm is used in the gain medium. In addition, a tight focus of about 4 µm radius on the SESAM is needed for sufficient saturation of the absorber [15]. The QML-threshold for the laser was at an output power of 2.8 mW. Above this value we achieved stable mode-locking with an optical efficiency of about 10% [24].

By systematically varying the design of the used SESAMs, thereby custom-tailoring the respective dispersion, we could again reduce the pulse duration by about 30% to get 1.1-ps pulses, at the cost of an output power reduction of about 14%. Figure 8 shows the calculated dispersion curves for the different SESAMs. Figure 9 shows the measured optical spectrum (top) and the autocorrelation trace (bottom). Compared to the result shown above, the reduced pulse duration and better temporal separation of the pulses is clearly visible. With additional improvements in the dispersion management for example by optimizing the group delay dispersion of the dielectric coating on the folding mirror, or with a Gires-Tournois interferometer structure included in the SESAM design [34], we expect the pulse duration to further decrease into the sub-picosecond regime. We have observed pulse durations of about 900 fs, but laser operation was not stable over time at this point.

### 2.4 Overview of achieved results

An overview of the results achieved to date by passively mode-locked high repetition rate Er,Yb:glass lasers is provided by the data of Table 1.

### 2.5 Transverse mode degeneracies in high repetition rate lasers

Cavity elements inside a laser resonator usually have a certain range with respect to their position along the optical axis, for which the resonator will be stable. For multi-GHz lasers the stability range of the SESAM, being used as an end-mirror, is in the order of few 100 µm. To obtain stable mode-locking, usually the SESAM has to be moved once within this range in order to find an optimum beam diameter on the device leading to the best saturation of the absorber. The stability range is usually limited on one end by the growing mode size in the gain, continuously raising the laser threshold. On the other end it is limited by the mode size on the SESAM approaching zero, which results in an unstable resonator. Within this range a rather smoothly varying laser output power is expected. However, we observed

**Table 1** Overview of results achieved with high repetition rate Er,Yb:glass lasers. $P_{av}$: average output power, $\tau_p$: pulse duration, TBP: time-bandwidth product, OSNR: optical signal-to-noise figure

| $f_{rep}$ [GHz] | Wavelength [nm] | $P_{av}$ [mW] | $\tau_P$ [ps] | TBP | OSNR [dB] | Ref. |
|---|---|---|---|---|---|---|
| 10 (10.67) | 1529–1569 | 15 | 3.8 | 0.47 (sech$^2$) | | [20] |
| 9.95328 | 1528–1563 | 30 | 1.2–1.9 | | >20 | [51] |
| 12.5 | 1528–1563 | 30 | 1.2–2.7 | | 40 | |
| 8.8–13.3 | 1533–1555 | 24 | 1.8 | 0.85 (Gauss) | | [28] |
| 25 | 1528–1561 | 25 | 1.9 | 0.75 | 30 | [29] |
| 40 | 1534 | 18 | 4.3 | 0.44 (Gauss) | 50 | [30] |
| 50 (49.87) | 1533 (?) | 7.5 | 2.1 | 0.57 (sech$^2$) | 65 | [27] |
| 77 | 1535.8 | 10.7 | 3.0 | 0.37 (sech$^2$) | 56 | [32] |
| 90 | 1535.3 | 10 | 4.1 | 0.42 (sech$^2$) | (58) | [33] |
| 101 | 1534.8 | 35 | 1.6 | 0.53 (sech$^2$) | 55 | [24] |
| 101 | 1534.2 | 30 | 1.1 | 0.39 (sech$^2$) | 55 | [52] |

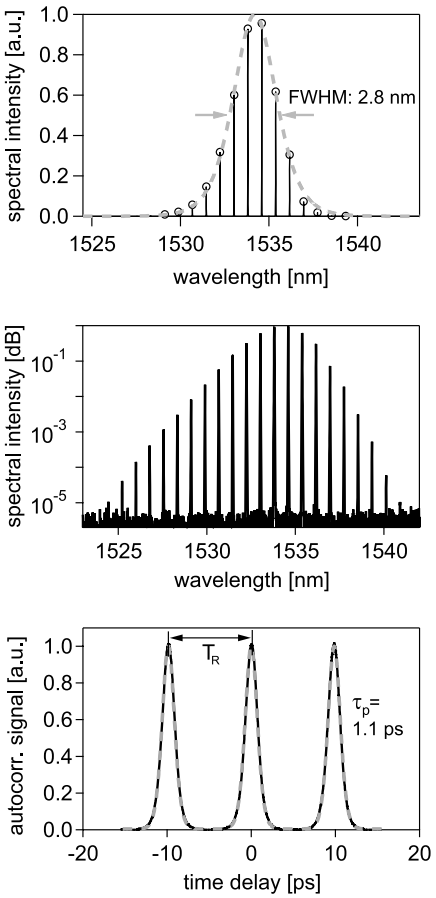


**Fig. 9** Properties of a 101-GHz laser, operated with an optimized SESAM: optical spectrum (*top, solid line*), together with an ideal sech$^2$ fit (*grey dashed line*). *Middle*: the optical spectrum on a logarithmic scale. *Bottom*: autocorrelation trace (*solid line*) with fit-curve using ideal sech$^2$ pulses (*grey dashed line*). Cavity roundtrip time $T_R = 9.84$ ps. The pulses have a duration of 1.1 ps

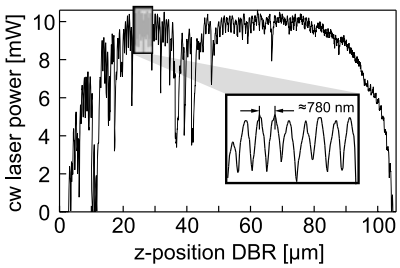


**Fig. 10** Stability range of cavity end-mirror z-position in a 100-GHz laser cavity. The cw output power is plotted versus the mirror position with a spatial resolution of approximately 40 nm. Large power drops and strong power oscillations are clearly visible. The *inset* shows the magnified power oscillations and their spatial period

multiple pronounced power drops while moving the SESAM within the stability range. When measuring the dependence between output power and end-mirror position in cw operation (in order to avoid Q-switched mode-locking instabilities) by scanning a high-reflecting mirror through the stability range with a spatial resolution of about 40 nm, we could observe that at certain distinct points, the output power drops significantly, as shown in Fig. 10. In addition, a comparably strong power oscillation is measured in cw operation.

Both observations are well reproducible over multiple scans and can be explained as follows: the amplitude oscillations on the measurement curve originate from the limited number of Fabry–Pérot modes of the laser cavity. An evaluation of 15 consecutive oscillations gives a period of 0.78 µm, which is approximately half the wavelength of the laser output. While varying the cavity length, the longitudinal cavity modes are moved through the gain profile, leading to power oscillations in the output.

The larger power drops have a different origin: it is well known from the literature that laser cavities in general exhibit frequency degeneracies of transverse cavity modes for certain resonator lengths within their stability range [35, 36]. For lasers designed to operate in the fundamental mode (TEM$_{00}$) this is particularly important, be-

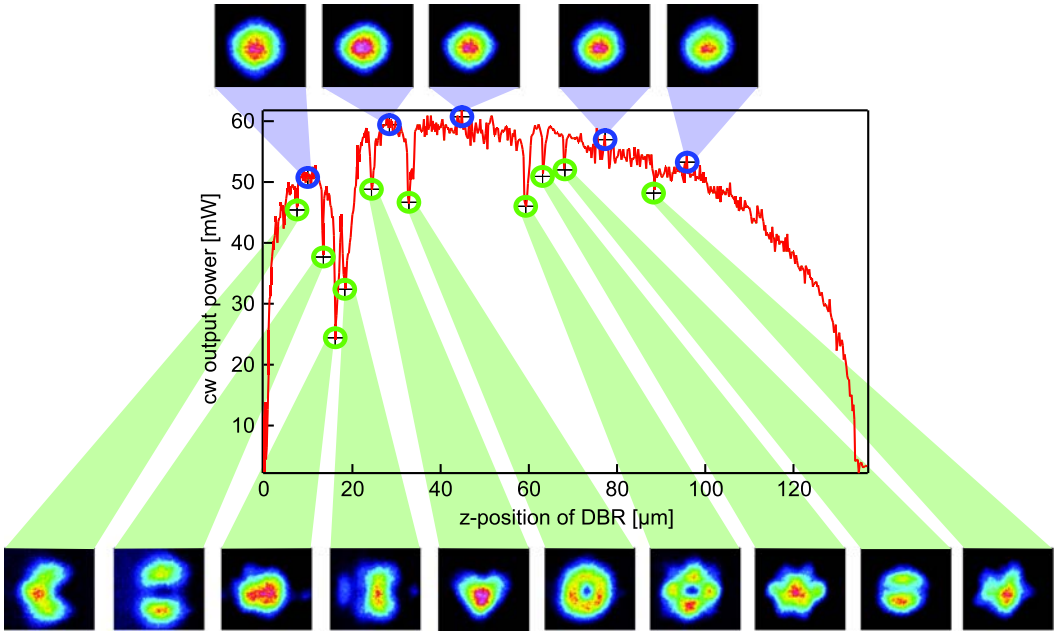


**Fig. 11** Stability range (with respect of the end-mirror position) of a 100 GHz laser cavity scanned in cw operation with a spatial resolution of 200 nm. The observed power drops can clearly be associated with strong beam quality degradations of the laser output. At normal power levels the output beam is diffraction limited

cause at such degeneracy points, higher order spatial modes can resonantly couple to the fundamental mode [37] and become predominant in the cavity. For a passively mode-locked laser this can lead to instabilities, as the SESAM is not sufficiently saturated by these modes anymore, and Q-switching can occur. When higher order spatial modes occur, they introduce an efficient power-loss channel, as some modes are quenched through effects of spatial hole burning in the inversion of the gain medium, leading to output power drops or even a complete laser shut-off. This is particularly distracting in a cavity with a very limited longitudinal stability range (with respect to the SESAM position) like in our case. For stable operation of high repetition rate mode-locked lasers, it is essential to accurately examine the cavity's stability range, as certain cavity lengths and their vicinity have to be avoided. To detect the beam quality deteriorations of a 100-GHz laser cavity we scanned the stability range again in cw operation with a more coarse resolution of about 200 nm (to reduce the overall measurement time) and recorded the output-power as well as the beam profile of the laser. Figure 11 again shows multiple large power drops within the stability range together with the associated beam profiles. In every power dip, the beam quality is clearly degraded, while at normal power levels, the output beam is nearly diffraction limited. The positions of the individual degeneracies are reproducible over multiple scans for a fixed particular pump power.

With varying pump power the positions slightly shift, as the changing thermal lens in the gain medium changes the resonator conditions. One should be aware of this effect if a laser is operated close to a degenerate point and the pump power is altered. In the measurement shown in Fig. 11 the above-mentioned power oscillations are not visible anymore, due to the reduced spatial resolution. Note that the absolute position of the individual power dips is different compared to those depicted in Fig. 10. The reason for these deviations are slight modifications of the laser cavity.

By modeling the laser cavity with ABCD matrix formalism one can calculate the position of the degeneracy points within the stability range. For a laser cavity which is radial-symmetric with respect to the intracavity laser mode, it is straightforward to calculate the resonance frequencies of Hermite-Gaussian laser modes with

$$\nu_{m,n,q} = \frac{c}{2L_{\text{eff}}}\left[q + (m+n+1)\frac{\cos^{-1}(\pm\sqrt{A_1 D_1})}{\pi}\right] \qquad (2)$$

$c$: speed of light, $L_{\text{eff}}$: effective optical resonator length, $q$: longitudinal mode number, $m, n$: transverse mode indices $\left|\begin{smallmatrix} A_1 & C_1 \\ B_1 & D_1 \end{smallmatrix}\right|$: single-pass cavity matrix, as described in [38]. Degeneracies arise where different cavity modes have the same frequency such that

$$\nu_{m+\Delta m,n+\Delta n,q+\Delta q} = \nu_{m,n,q}. \qquad (3)$$

The relative position of the intracavity optical elements is included in the cavity single-pass matrix. By inserting (2) into (3) we can solve for the position of the component we are interested in, which is included in $A_1 D_1$, resulting in the

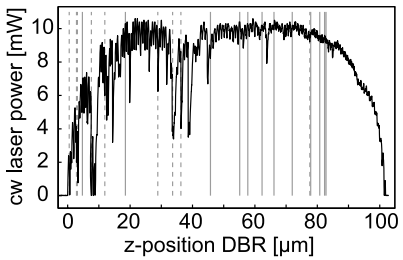


**Fig. 12** Comparison of measurement data (*black*) and theoretically calculated degeneracy points (*grey*) for $M$ and $N$ values reaching from one to ten. The *dashed grey lines* are in good agreement with the measured data while the *solid lines* cannot clearly be associated with specific power drops

degeneracy points of the cavity:

$$A_1 D_1 = \cos^2\left(\frac{-\Delta q}{\Delta m + \Delta n}\pi\right) = \cos^2\left(\frac{M}{N}\pi\right) \tag{4}$$

with $M = -\Delta q$ and $N = \Delta m + \Delta n$. For practical purposes usually only small values of $M$ and $N$ have to be considered, as the mode coupling strength decreases with increasing mode numbers [37]. We can see that all cavity related data in (2) are included in the term

$$\frac{\cos^{-1}(\pm\sqrt{A_1 D_1})}{\pi} \tag{5}$$

which is the Gouy phase shift of the electric field. By introducing any asymmetry into a laser resonator, as is done by inserting Brewster elements or tilted curved mirrors, one has to separately evaluate the tangential and the sagittal plane of the cavity. For the resulting optical resonance frequencies the Gouy phase shift of both planes contributes equally [39] such that we obtain

$$\nu_{m,n,q} = \frac{c}{2L_{\text{eff}}}\left[q + (m+n+1) \times \frac{\cos^{-1}(\pm\sqrt{A_{1,\text{tan}} D_{1,\text{tan}}}) + \cos^{-1}(\pm\sqrt{A_{1,\text{sag}} D_{1,\text{sag}}})}{2\pi}\right]. \tag{6}$$

Due to this modification it is not always trivial to solve (6) analytically. In this case numerical techniques should be used to calculate the degeneracy points. One should note that any misalignment or broken cavity symmetry (as in our cavities) will enhance the effective mode coupling such that higher order modes can couple to the fundamental mode and therefore reduce the beam quality [37].

Comparing measurement data with theoretically calculated degeneracy positions is rather difficult for a 100 GHz laser as many cavity parameters are not precisely know. Because we use a prism shaped gain glass, the effective gain length has a quite large uncertainty, effecting the position of all other cavity elements. Figure 12 shows such a comparison. The vertical grey lines represent the calculated positions. Some position are in a very good agreement with the measured power drops while others cannot clearly be related to some distinct measurement feature. Of course not every mode degeneracy has to result in a power drop, such that the beam quality could still be somewhat deteriorated in these points. Further experiments would be necessary to verify this.

## 3 Conclusion and outlook

In this paper we have reviewed the evolution of passively mode-locked 1.5 µm Er,Yb:glass lasers with record high repetition rates. Compared to other approaches operating at this wavelength, Er,Yb:glass lasers are an excellent alternative for generating high-quality picosecond pulses at multi-GHz repetition rates with relatively high output powers. Using different cavity designs, we demonstrated fundamentally mode-locked lasers with repetition rates ranging from 10 up to 100 GHz, which is to the best of our knowledge the highest repetition rate ever generated with a bulk laser in this spectral region. At this high repetition rate we have demonstrated average output powers of up to 35 mW and pulse durations as short as 1.1 ps.

Further, we have shown for the first time that beam quality deteriorations due to degenerate higher order spatial modes have to be considered when building a high repetition rate laser, as they can lead to instabilities during laser operation and even to a complete laser shut-off. In general, it is not possible to fully suppress degeneration effects in a laser cavity. To reduce the effective number of contributing modes, it is good practice to pump with a smooth and symmetric beam profile and to avoid misalignments and asymmetries inside the laser cavity, as for an ideal circular symmetry the coupling between the fundamental Gaussian mode and Hermite-Gaussian modes with an odd index will vanish and no energy will be transferred [37]. With the cavity single-pass matrix, it is possible to calculate the cavity configurations at which degeneracies occur. However, for high repetition rate laser cavities this is still difficult, as the geometric cavity parameters are usually not precisely known. They still can be determined experimentally, preferably in cw operation.

We believe that the current design approach does not allow for significant further increase in the repetition rate of Er,Yb:glass lasers, as the different components start to interfere and the dimensions of the individual components cannot be reduced much further. In the present 100-GHz setup, the clear aperture of the folding mirror is only about 400 µm. A further reduction of the diameter would lead to increasing diffraction losses and aberrations, reducing

the Q-factor of the cavity. Also the used gain length has a lower bound which is limited by the doping concentration of the active ions in the glass matrix. At Yb-doping levels above 25 wt-% ion clustering often appears [40]. Furthermore a too high doping concentration in the thermally poor conducting glass can lead to catastrophic failure due to fracture. A typical absorption length (1/e) of 0.5 mm requiring optical path lengths in the gain medium of 0.5–1 mm sets the lower limit to the cavity length and therefore limits the maximum achievable repetition rate to approximately 200 GHz. Fundamentally mode-locked lasers with pulse repetition rates between 100 and 200 GHz could be designed with monolithic cavity layouts. However, the main limiting factors are the small emission cross section of the gain glass and the saturation fluence of the SESAM, leading to a high QML threshold. In the spectral regime around 1 μm, where gain media with large gain cross sections are available, monolithic lasers with up to 160 GHz have been demonstrated [41]. However, this approach required equal mode sizes in the gain medium and on the saturable absorber. In the above reported Er,Yb:glass lasers the mode size ratio of gain element versus saturable absorber is typically in the order of 5, to achieve stable cw mode-locking. For a discussion of the influence of the gain material- and SESAM parameters it is helpful to rewrite (1) as

$$\left(\frac{P_{\text{intra}}}{f_{\text{rep}}}\right)^2 > F_{\text{sat,L}} A_{\text{eff,L}} F_{\text{sat,A}} A_{\text{eff,A}} \Delta R = \frac{h\nu}{\sigma_{\text{em}} + \sigma_{\text{abs}}} A_{\text{eff,L}} F_{\text{sat,A}} A_{\text{eff,A}} \Delta R. \quad (7)$$

In order to obtain a mode size ratio of 1 we have to increase the mode size on the saturable absorber. To maintain stable mode-locking we therefore need gain media with substantially higher interaction cross sections $\sigma_{\text{em}}$ and $\sigma_{\text{abs}}$ than Er,Yb:glass, or saturable absorbers with lower saturation fluence $F_{\text{sat,A}}$ than the used quantum-well SESAMs.

Recently new Er,Yb-doped crystalline materials with comparably high gain cross sections, improved thermal properties and very good optical quality have been reported together with corresponding laser results [42–44]. Also SESAMs based on quantum-dot (QD) absorbers (i.e. QD-SESAMs) are attractive and have been used to mode-lock semiconductor lasers [45, 46] and solid state lasers [47, 48]. With optimized growth conditions QD-SESAMs can exhibit very low saturation fluence which has been demonstrated in different spectral regimes [49, 50]. By varying the dot density, QD-SESAMs offer an additional degree of freedom to de-couple the modulation depth and the saturation fluence, such that both can then be custom tailored separately. If a mode size ratio of 1 can be achieved, monolithic high repetition rate solid state lasers could be assembled with bonding techniques, similar to those used for passively Q-switched microchip lasers emitting at 532 nm (like the ones used in early green laser pointers), reducing the complexity and the overall costs of the devices. Passively mode-locked GHz-sources could become a low-cost mass-product like green solid state laser pointers are today. For many applications they would be a high-performance but cost effective alternative to semiconductor based solutions.

**Acknowledgements** This work was supported by the European Commission through the Sixth Framework Programme MULTIWAVE (grant agreement 018074), the Seventh Framework Programme FAST-DOT (grant agreement 224338), and ETH Zurich with research grant TH-04 07-3 “Multiwave”.



## References

1. D.A.B. Miller, IEEE J. Sel. Top. Quantum Electron. **6**, 1312 (2000)
2. D.A.B. Miller, Opt. Lett. **14**, 146 (1989)
3. K.J. Weingarten, M.J.W. Rodwell, D.M. Bloom, IEEE J. Quantum Electron. **24**, 198 (1988)
4. H. Taga, M. Suzuki, Y. Namihira, Electron. Lett. **34**(22), 2098 (1998)
5. P. Bakopoulos, E. Kehayas, A.E.H. Oehler, T. Südmeyer, K.J. Weingarten, K.P. Hansen, U. Keller, H. Avramopoulos, An agile multi-wavelength optical source with configurable channel spacing and cw or pulsed operation for high-capacity WDM optical networks, in *Optical Fiber Communication Conference (OFC)*, San Diego, USA, 2009
6. M.C. Stowe, M.J. Thorpe, A. Pe’er, J. Ye, J.E. Stalnaker, V. Gerginov, S.A. Diddams (eds.) *Advances in Atomic, Molecular and Optical Physics*, vol. 55, ed. by E. Arimondo, P. Berman (Elsevier, Amsterdam, 2007)
7. S.A. Diddams, T. Udem, J.C. Bergquist, E.A. Curtis, R.E. Drullinger, L. Hollberg, W.M. Itano, W.D. Lee, C.W. Oates, K.R. Vogel, D.J. Wineland, Science **293**, 825 (2001)
8. M.T. Murphy, T. Udem, R. Holzwarth, A. Sizmann, L. Pasquini, C. Araujo-Hauk, H. Dekker, S. D’Odorico, M. Fischer, T.W. Hänsch, A. Manescau, Mon. Not. R. Astron. Soc. **380**, 839 (2007)
9. D.A. Braje, M.S. Kirchner, S. Osterman, T. Fortier, S.A. Diddams, Physics **48**(1), 57 (2008)
10. C.-H. Li, A.J. Benedick, P. Fendel, A.G. Glenday, F.X. Kartner, D.F. Phillips, D. Sasselov, A. Szentgyorgyi, R.L. Walsworth, Nature **452**(7187), 610 (2008)
11. E. Yoshida, N.. Shimizu, M.. Nakazawa, IEEE Photonics Technol. Lett. **11**(12), 1587 (1999)
12. K. Sato, IEEE J. Lightwave Technol. **20**(12), 2035 (2002)
13. U. Keller, A.C. Tropper, Phys. Rep. **429**(2), 67 (2006)
14. S. Lecomte, R. Paschotta, S. Pawlik, B. Schmidt, K. Furusawa, A. Malinowski, D.J. Richardson, U. Keller, IEEE Photonics Technol. Lett. **17**, 483 (2005)
15. U. Keller, Nature **424**, 831 (2003)
16. U. Keller, D.A.B. Miller, G.D. Boyd, T.H. Chiu, J.F. Ferguson, M.T. Asom, Opt. Lett. **17**, 505 (1992)
17. U. Keller, K.J. Weingarten, F.X. Kärtner, D. Kopf, B. Braun, I.D. Jung, R. Fluck, C. Hönninger, N. Matuschek, J. Aus der Au, IEEE J. Sel. Top. Quantum Electron. **2**(3), 435 (1996)

18. H.A. Haus, IEEE J. Quantum Electron. **12**, 169 (1976)
19. C. Hönninger, R. Paschotta, F. Morier-Genoud, M. Moser, U. Keller, J. Opt. Soc. Am. B **16**(1), 46 (1999)
20. L. Krainer, R. Paschotta, G.J. Spühler, I. Klimov, C.Y. Teisset, K.J. Weingarten, U. Keller, Electron. Lett. **38**(5), 225 (2002)
21. A. Schlatter, S.C. Zeller, R. Grange, R. Paschotta, U. Keller, J. Opt. Soc. Am. B **21**(8), 1469 (2004)
22. R. Grange, M. Haiml, R. Paschotta, G.J. Spuhler, L. Krainer, M. Golling, O. Ostinelli, U. Keller, Appl. Phys. B **80**(2), 151 (2005)
23. G.J. Spühler, K.J. Weingarten, R. Grange, L. Krainer, M. Haiml, V. Liverini, M. Golling, S. Schon, U. Keller, Appl. Phys. B **81**(1), 27 (2005)
24. A.E.H. Oehler, T. Südmeyer, K.J. Weingarten, U. Keller, Opt. Express **16**(26), 21930 (2008)
25. T.R. Schibli, E.R. Thoen, F.X. Kärtner, E.P. Ippen, Appl. Phys. B **70**(Suppl.), S41 (2000)
26. R. Grange, *Near Infrared Semiconductor Saturable Absorber Mirrors for High Repetition Rate Lasers*, ed. by H. Baltes et al. Series in Quantum Electronics (Hartung-Gorre, Konstanz, 2006)
27. S.C. Zeller, L. Krainer, G.J. Spühler, R. Paschotta, M. Golling, D. Ebling, K.J. Weingarten, U. Keller, Electron. Lett. **40**(14), 875 (2004)
28. C. Erny, G.J. Spähler, L. Krainer, R. Paschotta, K.J. Weingarten, U. Keller, Electron. Lett. **40**(14), 877 (2004)
29. G.J. Spühler, P.S. Golding, L. Krainer, I.J. Kilburn, P.A. Crosby, M. Brownell, K.J. Weingarten, R. Paschotta, M. Haiml, R. Grange, U. Keller, Electron. Lett. **39**(10), 778 (2003)
30. S.C. Zeller, L. Krainer, G.J. Spühler, K.J. Weingarten, R. Paschotta, U. Keller, Appl. Phys. B **76**(7), 1181 (2003)
31. G.J. Spühler, L. Krainer, E. Innerhofer, R. Paschotta, K.J. Weingarten, U. Keller, Opt. Lett. **30**(3), 263 (2005)
32. S.C. Zeller, T. Südmeyer, K.J. Weingarten, U. Keller, Electron. Lett. **43**(1), 32 (2007)
33. A.E.H. Oehler, S.C. Zeller, T. Südmeyer, U. Keller, K.J. Weingarten, in *Conference on Lasers and Electro-Optics (Europe)* (IEEE, Munich, 2007)
34. D. Kopf, G. Zhang, R. Fluck, M. Moser, U. Keller, Opt. Lett. **21**, 486 (1996)
35. J.A. Arnaud, Appl. Opt. **8**, 189 (1969)
36. Q. Zhang, B. Ozygus, H. Weber, Eur. Phys. J. A **6**, 293 (1999)
37. R. Paschotta, Opt. Express **14**(13), 6069 (2006)
38. O. Svelto, *Principles of Lasers*, 4th edn. (Plenum, New York), p. 647
39. A.E. Siegman, *Lasers*, ed. by A. Kelly (University Science Books, Mill Valley, 1986)
40. S. Jiang, M. Myers, N. Pezghambarian, J. Non-Cryst. Solids **239**, 143 (1998)
41. L. Krainer, R. Paschotta, S. Lecomte, M. Moser, K.J. Weingarten, U. Keller, IEEE J. Quantum Electron. **38**(10), 1331 (2002)
42. J. Li, J. Wang, H. Tan, H. Zhang, F. Song, S. Zhao, J. Zhang, X. Wang, Mater. Res. Bull. **39**, 1329 (2004)
43. Y.J. Chen, Y.F. Lin, X.H. Gong, Q.G. Tan, Z.D. Luo, Y.D. Huang, Appl. Phys. Lett. **89**(24), 241111 (2006)
44. A.A. Lagatsky, V.E. Kisel, A.E. Troshin, N.A. Tolstik, N.V. Kuleshov, N.I. Leonyuk, A.E. Zhukov, E.U. Rafailov, W. Sibbett, Opt. Lett. **33**(1), 83 (2008)
45. A. Garnache, S. Hoogland, A.C. Tropper, J.M. Gerard, V. Thierry-Mieg, J.S. Roberts, Pico-second passively mode locked surface-emitting laser with self-assembled semiconductor quantum dot absorber, in *CLEO/Europe-EQEC*, 2001
46. E.U. Rafailov, S.J. White, A.A. Lagatsky, A. Miller, W. Sibbett, D.A. Livshits, A.E. Zhukov, V.M. Ustinov, IEEE Photonics Technol. Lett. **16**(11), 2439 (2004)
47. C. Scurtescu, Z.Y. Zhang, J. Alcock, R. Fedosejevs, M. Blumin, I. Saveliev, S. Yang, H. Ruda, Y.Y. Tsui, Appl. Phys. B **87**(4), 671 (2007)
48. M. Lumb, D. Farrell, E. Clarke, M. Damzen, R. Murray, Appl. Phys. B **94**(3), 393 (2009)
49. J. Inoue, T. Isu, K. Akahane, N. Yamamoto, M. Tsuchyida, Phys. Status Solidi **3**, 520 (2006)
50. D.J.H.C. Maas, A.R. Bellancourt, M. Hoffmann, B. Rudin, Y. Barbarin, M. Golling, T. Südmeyer, U. Keller, Opt. Express **16**(23), 18646 (2008)
51. Datasheet ERGO-XG, GigaTera Pulse-Generating Laser (2007)
52. A.E.H. Oehler, T. Südmeyer, K.J. Weingarten, U. Keller, 100 GHz passively mode-locked Er:Yb:glass laser at 1.5 μm and experimental identification of transverse cavity-mode degeneracies, in *Advanced Solid-State Photonics (ASSP)*, Denver, USA, 2009